ELSEVIER

Journal of Biomechanics 39 (2006) 603–616

JOURNAL OF BIOMECHANICS

www.elsevier.com/locate/jbiomech
www.JBiomech.com

Analysis of the mechanical behavior of chondrocytes in unconfined compression tests for cyclic loading

John Z. Wu[a,b,*], Walter Herzog[b]

[a]National Institute for Occupational Safety and Health, Morgantown, West Virginia, USA
[b]The University of Calgary, Calgary, Alberta, Canada

Accepted 16 January 2005

Abstract

Experimental evidence indicates that the biosynthetic activity of chondrocytes is associated with the mechanical environment. For example, excessive, repetitive loading has been found to induce cell death, morphological and cellular damage, as seen in degenerative joint disease, while cyclic, physiological-like loading has been found to trigger a partial recovery of morphological and ultrastructural aspects in osteoarthritic human articular chondrocytes. Mechanical stimuli are believed to influence the biosynthetic activity via the deformation of cells. However, the in situ deformation of chondrocytes for cyclic loading conditions has not been investigated experimentally or theoretically. The purpose of the present study was to simulate the mechanical response of chondrocytes to cyclic loading in unconfined compression tests using a finite element model. The material properties of chondrocytes and extracellular matrix were considered to be biphasic. The time-histories of the shape and volume variations of chondrocytes at three locations (i.e., surface, center, and bottom) within the cartilage were predicted for static and cyclic loading conditions at two frequencies (0.02 and 0.1 Hz) and two amplitudes (0.1 and 0.2 MPa). Our results show that cells at different depths within the cartilage deform differently during cyclic loading, and that the depth dependence of cell deformation is influenced by the amplitude of the cyclic loading. Cell deformations under cyclic loading of 0.02 Hz were found to be similar to those at 0.1 Hz. We conclude from the simulation results that, in homogeneous cartilage layers, cell deformations are location-dependent, and further are affected by load magnitude. In physiological conditions, the mechanical environment of cells are even more complex due to the anisotropy, depth-dependent inhomogeneity, and tension-compression non-linearity of the cartilage matrix. Therefore, it is feasible to speculate that biosynthetic responses of chondrocytes to cyclic loading depend on cell location and load magnitude.
Published by Elsevier Ltd.

Keywords: Biphasic; Poroelastic; Cartilage; Finite element analysis; Cell mechanics; Cyclic loading

1. Introduction

Experimental evidence indicates that cells are sensitive to their mechanical (stress–strain) state, and react directly to mechanical stimuli. The biosynthetic response of chondrocytes was found to be sensitive to the frequency and amplitude of loading (Wong et al., 1999; Kurz et al., 2001). Recent experimental studies further indicate that excessive, repetitive loading may induce cell death, and cause morphological and cellular damage, as seen in degenerative joint disease (Lucchinetti et al., 2002; Sauerland et al., 2003). Islam et al. (2002) found that continuous cyclic hydrostatic pressure (5 MPa, 1 Hz for 4 h) induced apoptosis in human chondrocytes derived from osteoarthritic cartilage in vitro. In contrast, cyclic, physiological-like loading was found to trigger a partial recovery of morphological and ultrastructural aspects in osteoarthritic human articular chondrocytes (Nerucci et al., 1999).

Chondrocyte deformation during cartilage loading is rarely analysed experimentally. Guilak (1995) compared

*Corresponding author. National Institute for Occupational Safety and Health, 1095 Willowdale Road, MS 2027, Morgantown, WV 26505, USA. Tel.: +1 304 285 5832; fax: +1 304 285 6265.
E-mail address: jwu@cdc.gov (J.Z. Wu).

0021-9290/$ - see front matter Published by Elsevier Ltd.
doi:10.1016/j.jbiomech.2005.01.007

chondrocyte nucleus deformations in 11 cells in an unloaded configuration to those in a loaded, steady-state (15% compression) configuration using confocal laser scanning microscopy. Similarly, Buschmann et al. (1995) presented data of chondrocyte deformation for fixed articular cartilage specimens from the patellofemoral groove of 1–2 week old calves. Cell and nuclear volume, vertical radius, and surface areas were given for four static loading conditions using cartilage explants and unconfined compression. Guilak et al. (1995) presented chondrocyte deformations for 18 cells from the surface, middle and deep zone of a cartilage specimen for a single loading condition. Elder et al. (2001) studied the effects of dynamic compressive loading on chondrocyte differentiation in vitro. In their study, cells embedded in agarose gel were subjected to uniaxial, cyclic compressions at 0.03, 0.15, or 0.33 Hz for 2 h. They found a significant increase in chondrocyte differentiation under cyclic loading, and concluded that cells were sensitive to the level of cumulative (non-recoverable) compressive strain, as well as to the dynamic strain history. It was assumed that the cells sense their mechanical environment mainly via deformation (Buschmann et al., 1995; Guilak, 1995). More recently, Clark et al. (2003) studied deformations of chondroyctes in feline patellofemoral joint under physiological compressive loading. They found that for a given compressive load, the shape and volume of chondrocytes at different locations of an intact articular cartilage specimen, attached to its native bone, were different. Knight et al. (1998) studied the deformation patterns of isolated chondrocytes in agarose in cyclic compression. They examined the time-histories of the shape variations of chondrocytes. The time-dependent variations of volume, stress/strain, and interstitial fluid pressure in chondrocytes for cyclic loading conditions have not been studied experimentally or theoretically to date.

Chondrocytes receive mechanical stimuli via interactions with the surrounding intercellular matrix. Parkkinen et al. (1993) tested primary chondrocyte cell cultures and explants of bovine articular cartilage under cyclic hydrostatic pressure. They found that cyclic hydrostatic pressures of physiological magnitude had a significant influence on proteoglycan synthesis. Giannoni et al. (2003) found that the expression of cartilage oligomeric matrix protein (COMP) was sensitive to long term cyclic compression in calf articular cartilage explants and cylindrical alginate/chondrocyte constructs. They found that COMP transcript was significantly enriched upon compression in both experimental systems, and that cell/matrix interactions were the key events in mechanotransduction in chondrocytes.

Fluid pressure and stress–strain state in and around chondrocytes are important mechanical stimuli associated with remodeling, adaptation, and degeneration of articular cartilage. Experimental studies have indicated that cyclic compressive loads have more pronounced effects on the biosynthetic activity of cells than static compression loads. Experimental studies on the deformation behavior of chondrocytes to date were usually carried out using confined or unconfined compression tests. In unconfined tests, the cartilage samples are usually attached to the subchondral bone and squeezed between permeable or impermeable platens. The lateral sides of the cartilage specimens are not restrained for displacement and fluid flow. In this case, the cartilage specimen is not deformed in a uniform, one-dimensional compression. Consequently, deformation of chondrocytes does not only depend on the rate of cartilage deformation, but also on the location of cells within the specimen and the fluid boundary conditions of the compression platen. However, only the overall response of cartilage to dynamic loading has been observed in the experiments to date. The deformation behavior of chondrocytes in articular cartilage does not only depend on the state of loading but also on cell location. These complex time- and location-dependent cell deformations have not been investigated experimentally. The purpose of the present study was to simulate numerically the location- and time-dependent stress–strain state and fluid pressure distribution in chondrocytes in an unconfined, cyclic compression test.

2. Methods

2.1. Finite element simulations

It is technically difficult to precisely simulate the time-dependent stress and strain state of individual cells at different locations within articular cartilage, including the coupling effects of the distributed chondrocytes. In this study, we used a numerical mixture technique to overcome this difficulty (Wu et al., 1999; Wu and Herzog, 2000). Cartilage was considered to be composed of an extracellular matrix and small, spherical cells that were randomly distributed in the matrix. The theoretical approach involved three basic steps: first, the cartilage was approximated as a macroscopically homogenized material having effective material properties; second, the averaged mechanical behavior of cartilage was obtained using the homogenized model; and third, the solution of the time-dependent displacement and fluid pressure fields was used as the time-dependent boundary conditions for a microscopic sub-model, to obtain the average, time-dependent mechanical behavior of cells in different locations within the cartilage. Matrix and cells were treated as biphasic materials (Mow et al., 1980). Permeability was assumed to be deformation-dependent (Holmes, 1986).

The commercial finite element software ABAQUS (version 6.3) was used for all simulations. Large deformation theory with updated Lagrangian strains was applied in all simulations.

Numerical tests using unconfined compression with similar configurations as in the experiments by Guilak et al. (1995) were performed. The cartilage specimen was cylindrical, had a thickness of 1.0 mm and a diameter of 6.0 mm (Fig. 1a). The specimen was assumed to be unconfined at the lateral boundary and to be bound perfectly at the bottom by a rigid, impermeable plate, simulating the cartilage–bone interface. The compression platen on top of the specimen was assumed to be rigid and impermeable. The contact between the compression plate and the cartilage specimen was assumed to be frictionless.

Cells were assumed to have an original diameter, $2R$, of 20 μm in all tests and analyses of three cells located at different positions within the cartilage specimen were performed (Fig. 1a): A($r = 0$ mm, $z = 0$ mm), B($r = 0$ mm, $z = 0.4$ mm), and C($r = 0$ mm, $z = -0.4$ mm).

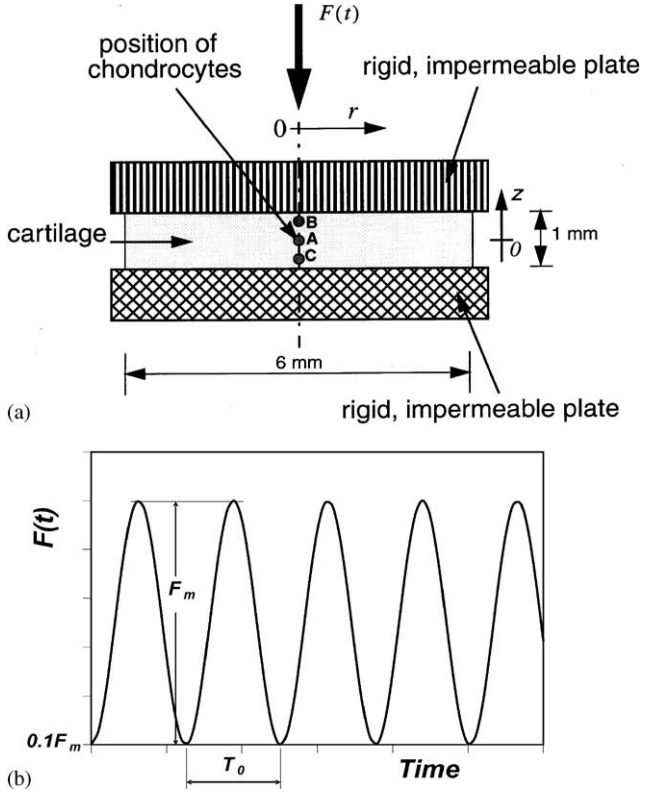

Fig. 1. Model of numerical tests: (a) unconfined compression test with impermeable compression plate; (b) time history of the applied loading during numerical simulations. The cartilage specimen is cylindrical, has a thickness of 1 mm and a diameter, D, of 6 mm. The interface between cartilage and the bottom plate was assumed to be perfectly bound, and the contact between cartilage and the top plate was assumed to be smooth. The chondrocytes of interest were assumed to have an initial diameter 20 μm and to be located at A(0.0,0.0), B(0.0,0.40), and C(0.0,−0.40). [coordinates in mm].

The numerical tests were carried out using a force-controlled protocol. The specimen was subjected to a cyclic load (Fig. 1b):

$$F(t) = \frac{F_m}{2}\left[1 - \cos\left(\frac{2\pi t}{T_0}\right)\right] + 0.10\,F_m, \tag{1}$$

where t is the time; T_0 is the cycle period ($f = 1/T_0$); and F_m is the load-cycling amplitude that is related to the average pressure-cycling amplitude, p_m, by $F_m = p_m(\pi D^2/4)$ with D being the diameter of the specimen.

The effects of load frequency and amplitude on cell deformation were investigated using unconfined compression tests at three frequencies and two amplitudes (i.e., $f = 0$, 0.02, and 0.10 Hz; $p_m = 0.1$ and 0.2 MPa). Zero frequency (i.e., $T_0 \to \infty$ or $f = 0$ Hz) corresponds to a constant load. The magnitude of the constant load was $F(t) = F_{\text{constant}} = 0.60\,F_m + 0.10\,F_m = 0.7\,F_m$ ($p(t) = 0.70\,p_m$), the average value for one loading cycle.

2.2. Model parameters

The values for the elastic modulus (E), Poisson's ratio (ν), and the initial permeability (k) of the matrix and cell were taken from experimental measurements (Athanasiou et al., 1991; Jones et al., 1997; Shin and Athanasiou, 1997): $E_m = 0.50$ MPa, $\nu_m = 0.1$, $k_m^0 = 1.0 \times 10^{-15}$ m^4/Ns, $E_c = 0.50$ kPa, $\nu_c = 0.4$, and $k_c^0 = 1.0 \times 10^{-10}$ m^4/Ns, with subscripts m and c designating matrix and cell material, respectively.

A typical cell volumetric fraction was assumed to be 5% (Stockwell, 1979). Using the mixture model (Wu et al., 1999), the effective elastic modulus, Poisson's ratio, and the initial permeability of the homogenized cartilage matrix were determined to be $E = 0.45$ MPa, $\nu = 0.106$, and $k_0 = 1.16 \times 10^{-15}$ m^4/Ns, respectively.

The initial volume fraction of the solid phase within the cells and the matrix were assumed to be 5% and 20%, respectively ($\Phi_0^{s(c)} = 0.05$, $\Phi_0^{f(c)} = 0.95$, $e_0^c = 19.0$; $\Phi_0^{s(m)} = 0.20$, $\Phi_0^{f(m)} = 0.80$, $e_0^m = 4.0$). The initial void ratio of the homogenized cartilage matrix was estimated by

$$e_0^{\text{effective}} = \frac{\Phi_0^{f(c)}c + \Phi_0^{f(m)}(1-c)}{\Phi_0^{s(c)}c + \Phi_0^{s(m)}(1-c)}. \tag{2}$$

The deformation dependence of the permeabilities for the cells, matrix and the homogenized cartilage in the deformed states was assumed to be exponential (Wu and Herzog, 2000):

$$k = k_0\left(\frac{e}{e_0}\right)^{\kappa}\exp\left\{\frac{M}{2}\left[\left(\frac{1+e}{1+e_0}\right)^2 - 1\right]\right\}, \tag{3}$$

where material parameters M and κ have been determined previously (Holmes, 1986) to be 4.638 and 0.0848, respectively.

Large deformation theory with updated Lagrangian strains was applied in all simulations. Elastic stress of the solid phase (in matrix and cells) for finite deformation was defined using a hyperelastic constitutive relation

$$\sigma_i^e = \frac{\partial U}{\partial \lambda_i} \qquad i = 1,2,3, \tag{4}$$

$$U = \sum_{i=1}^{N} \frac{2\mu_i}{\alpha_i^2}\left[\lambda_1^{\alpha_i} + \lambda_2^{\alpha_i} + \lambda_3^{\alpha_i} - 3 + \frac{1}{\beta}\left((J)^{-\alpha_i\beta} - 1\right)\right], \tag{5}$$

where σ_i^e and λ_i $(i = 1,2,3)$ are the principal elastic stresses and the principal stretch ratios, respectively; U is the strain energy function; $J = \lambda_1\lambda_2\lambda_3$ is the volume ratio; α_i, μ_i $(i = 1,\ldots,N)$, and β are material parameters.

The initial shear modulus, μ, and the initial bulk modulus, K, were related to the material parameters in Eq. (5) by

$$\mu = \sum_{i=1}^{N} \mu_i, \quad K = \sum_{i=1}^{N} 2\left(\frac{1}{3} + \beta\right)\mu_i, \quad \beta = \frac{v}{1-2v}. \tag{6}$$

The material parameters α_i and μ_i $(i = 1,\ldots,N)$ were obtained by fitting Eq. (5) to uniaxial stress–strain curves. Matrix and cells were assumed to have a linear stress–strain relation at strains less than a specified limit, ε_m ($\varepsilon_m = 0.30, 0.50$ for matrix and cells, respectively). Further deformation resulted in an increasing stiffness (Ateshian et al., 1997). In an infinitesimal strain range, Eqs. (4) and (5) are equivalent to Hooke's law. In order to obtain a best fitting curve with less than a 1% relative error, a five-term form ($N = 5$) of Eq. (5) was used.

3. Results

The time-histories of the normalized volumetric variations of chondrocytes at three locations (i.e., surface, center, and bottom) within the cartilage specimen were predicted for cyclic loading at two different frequencies ($f = 0.02$ and 0.1 Hz) and two amplitudes ($p_m = 0.1$ and 0.2 MPa) (Figs. 2 and 3). The normalized volumetric changes of the central cell for static loading (i.e., $f = 0$) are also shown in these figures (Figs. 2c and 3c). Generally, the amplitude of the cyclic volumetric variation of the cells was not changing with time (Figs. 2 and 3), while the average cell volume decreased as a function of time for static and cyclic loading (Figs. 2c and 3c). The cell volumetric variations increased dramatically with increasing cyclic loading amplitude.

Our results show that the cells at different depths within the cartilage deform differently during the cyclic loading, and that the depth dependence of the cell deformations is influenced by the amplitude of the cyclic loading. For small cycling amplitudes ($p_m = 0.1$ MPa), the cell near the "bone–cartilage interface" (cell C, Fig. 1a) experienced larger deformations (larger cyclic amplitudes) than the cells at the center (cell A, Fig. 1a) and near the contact surface (cell B, Fig. 1a) (Figs. 2a and b). For large cycling amplitudes ($p_m = 0.2$ MPa), the cell at the center experienced larger cyclic deformation amplitudes than the cells at the bottom and near the contact surface (Figs. 3a and b).

The normalized volumetric variations of the central cell under different cycling frequencies ($f = 0$, 0.02, and 0.1 Hz) and amplitudes ($p_m = 0.1$ and 0.2 MPa) indicate that cell deformation is independent of the loading frequency (Figs. 2c and 3c), at least for the frequencies simulated here.

In order to study the effects of loading frequency and cycle amplitude on deformation of cells at different depths, variations in normalized cell height, width, and volume at time 1000 s, and during one loading period were compared (Figs. 4 and 5).

For small cyclic loading ($p_m = 0.1$ MPa), variations in cell height were independent of depth (Figs. 4a and b), while cell width was depth-dependent (Figs. 4c and d). The depth-dependent, cyclic variations of cell volume were mainly due to the variations in cell height (Figs. 4e and f). Cell shape became flatter (width increased, as shown in Figs. 4c and d) and cells were depressed more (volume decreased, as shown in Figs. 4e and f) in the deep zone (near cartilage-bone interface) compared to the surface zone.

At high cycle amplitudes (i.e., $p_m = 0.2$ MPa, Fig. 5), variations in cell shape and volume were significantly greater than those observed at the small amplitude (i.e., $p_m = 0.1$ MPa, Fig. 4). It is interesting to note that, at the instant of peak loading (i.e., period = 0.5), cells in the surface zone deform the least, while cells at the center deform the most. By comparing Figs. 5 and 4, it becomes apparent that cell deformation in the center zone increases more rapidly with increasing loads than that for cells in the surface or the deep zone.

Comparing results obtained at loading frequencies of 0.1 and 0.02 Hz (i.e., Figs. 4a,c,e vs. Figs. 4b,d,f and Figs. 5a,c,e vs. Figs. 5b,d,f, respectively), it becomes obvious that variations in height, width, and volume of cells are similar, indicating that loading frequency has a negligible effect on cell deformation behavior, at least for the frequencies used here.

In order to study the time-histories of cell deformation in different layers of the cartilage, variations in normalized cell volume during a cycle period for the two loading levels were analyzed. For the small load ($p_m = 0.1$ MPa, Figs. 6a,c,e), the normalized cell volume decreased with increasing time during a time period of 800 s. For the large load ($p_m = 0.2$ MPa, Figs. 6b,d,f), the peak value of the normalized cell volume changed little after 200 s of cycling.

Fluid pressures increased slightly from the surface to the deep zone (5% for $p_m = 0.1$ MPa and 10% for

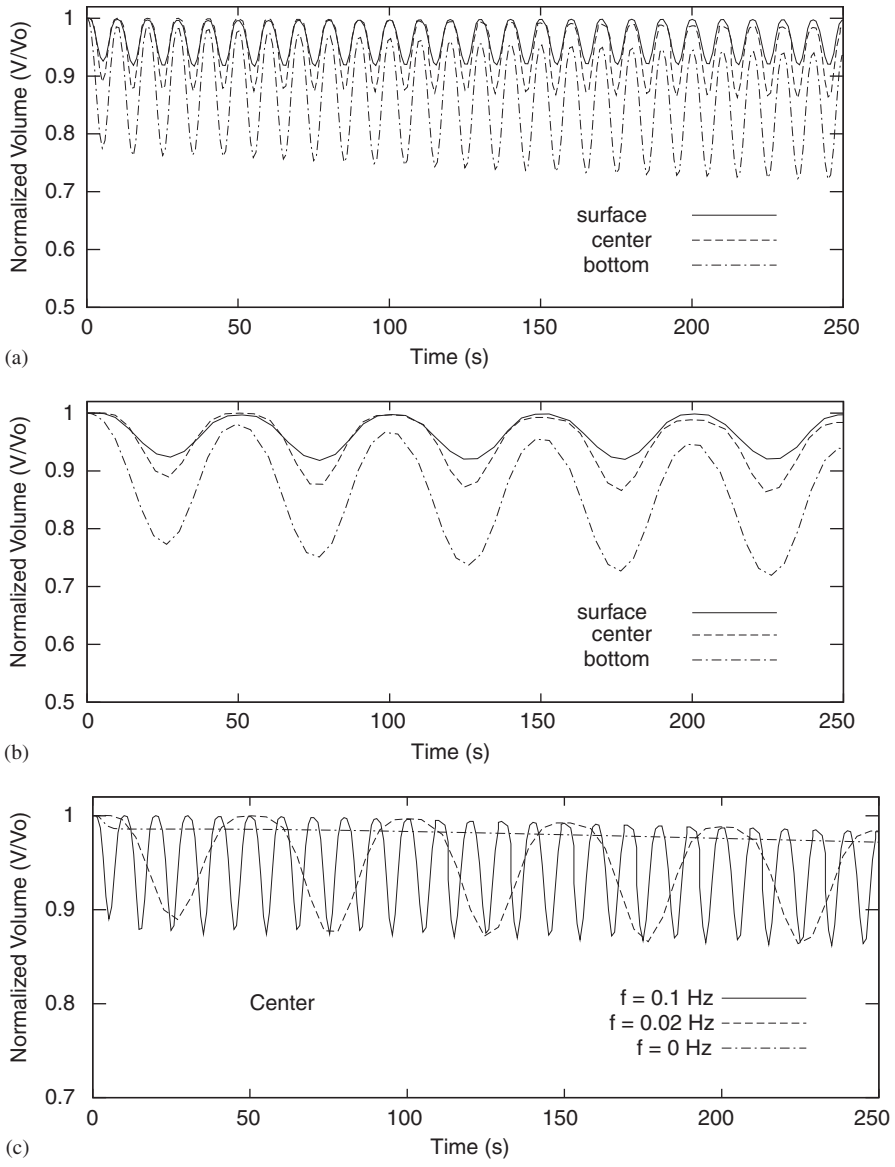

Fig. 2. Time histories of normalized volumetric variations of chondrocytes for cyclic loading: $p_m = 0.1$ MPa. (a) $f = 0.1$ Hz, three cell locations; (b) $f = 0.02$ Hz, three cell locations; (c) $f = 0.0, 0.02$, and 0.1 Hz, cell at center. The cell volume as a function of time was normalized relative to that in the undeformed state, V_0.

$p_m = 0.2$ MPa); and fluid pressure gradients across the cartilage thickness increased with increasing pressure magnitude (Fig. 7). The peak fluid pressure during a cycle increased for approximately 200 s, then decreased with increasing cycling time. For $p_m = 0.1$ MPa (Figs. 7a,c,e), the peak fluid pressure across the cartilage layer decreased with increasing time for the entire simulation period (800 s). For $p_m = 0.2$ MPa (Figs. 7b,d,f), the peak fluid pressure in the deep zone decreased with increasing cycling time and reached a steady-state at approximately 800 s, while the peak fluid pressure in the center and surface zone decreased with increasing cycling time and did not reach steady-state values up to 800 s.

The time-histories of the normalized height, normalized width, normalized volume, and fluid pressure of cells in the surface, center, and deep zones under constant compression are illustrated in Fig. 8. The simulations were performed using a constant pressure of 0.14 MPa ($p = 0.7\,p_m$, with $p_m = 0.2$ MPa). The changes in cell shape, volume, and fluid pressure at $t = 0$ were caused by the suddenly applied load. The cell in the deep zone experienced greater shape change and volumetric variations than the cells in the surface and center zone (Figs. 8a–c). Immediately after application of the compressive loading, there was a fluid pressure gradient across the cartilage thickness: the fluid pressure increased from the surface to the deep zone (Fig. 8d), and

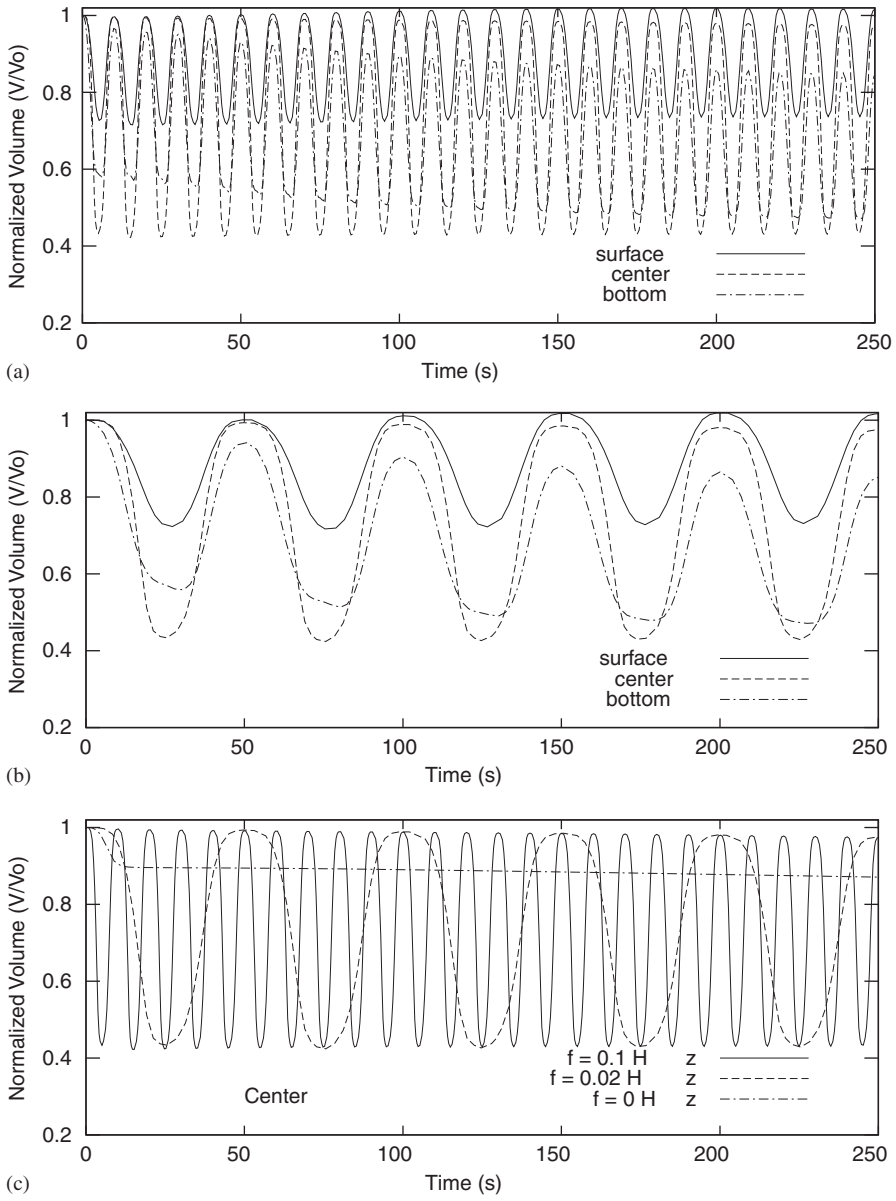

Fig. 3. Time histories of normalized volumetric variations of chondrocytes for cyclic loading: $p_m = 0.2$ MPa. (a) $f = 0.1$ Hz, three cell locations; (b) $f = 0.02$ Hz, three cell locations; (c) $f = 0.0, 0.02$, and 0.1 Hz, cell at center. The cell volume as a function of time was normalized relative to that in the undeformed state, V_0.

the fluid pressure gradient tended to decrease with increasing time.

4. Discussion and conclusion

Experimental evidence suggests that the biosynthetic activity of chondrocytes is associated with, and possibly regulated by, the mechanical environment. The response of isolated, in vitro chondrocytes to static and dynamic mechanical loading has been studied experimentally. It is still technically difficult to continuously monitor the variations of volume, stress/strain, and interstitial fluid pressure in chondrocytes during cyclic loadings to date. Therefore, numerical simulations are effective means to study the variable chondrocyte mechanics in an in vivo or in situ cartilage specimen. The present analysis shows for the first time the depth- and time-dependent deformation behavior of chondrocytes under cyclic loading at two different loading frequencies and cycle amplitudes. These simulation results may be useful in exploring the possible mechanisms of initiation and development of osteoarthritis.

In vitro tests of articular cartilage under cyclic loading were typically performed using cartilage explants via (confined or unconfined) compression tests

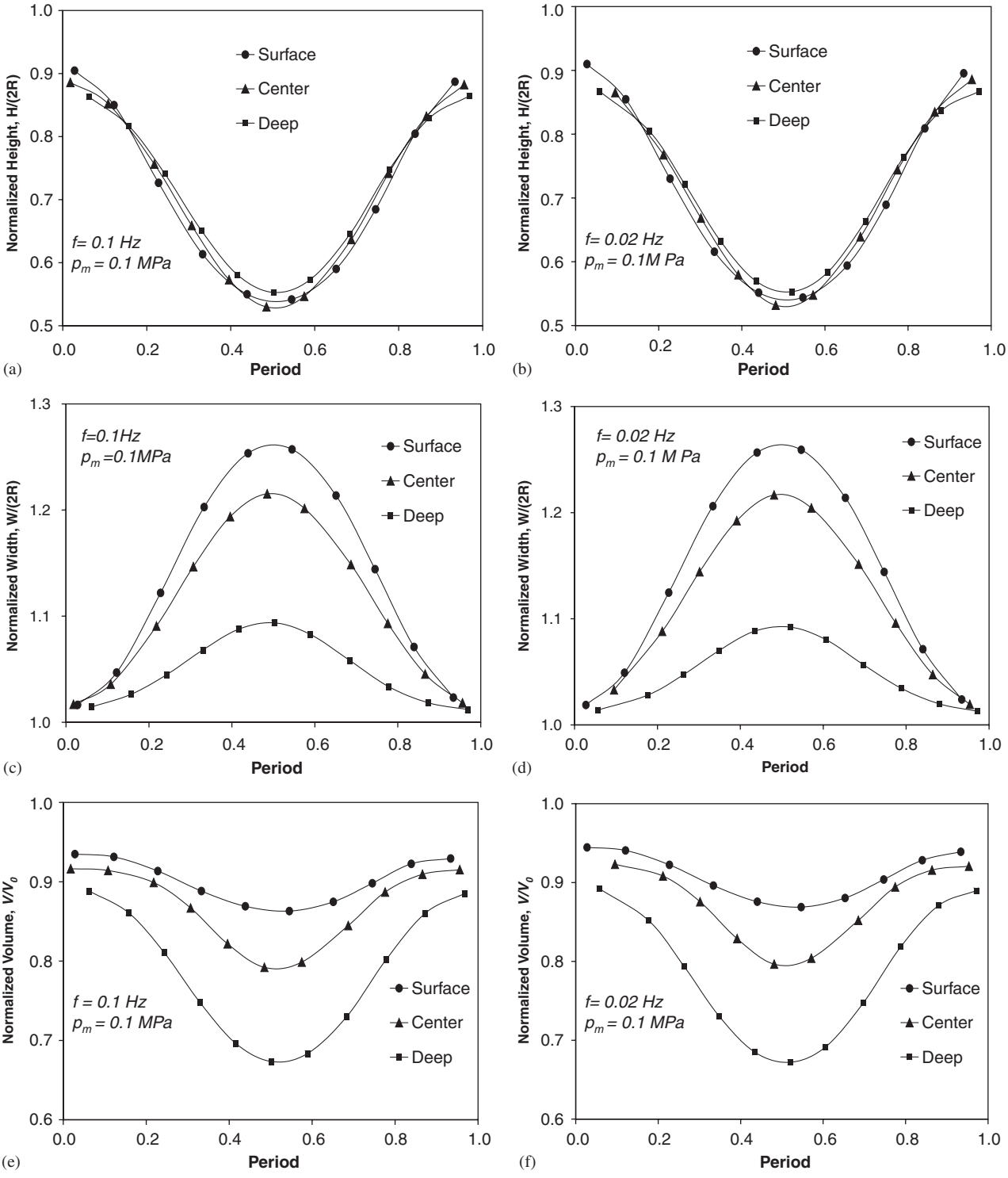

Fig. 4. Variations in cell shape for cyclic loading at $t = 1000$ s: $p_m = 0.1$ MPa. (a) and (b): normalized cell height, $f = 0.1$ and 0.02 Hz; (c) and (d): normalized cell width, $f = 0.1$ and 0.02 Hz; (e) and (f): normalized cell volume, $f = 0.1$ and 0.02 Hz. The cell volume as a function of time was normalized relative to that in the undeformed state, V_0; the cell height and cell width as a function of time was normalized relative to the cell diameter in the undeformed state, $2R$.

(e.g., Parkkinen et al., 1993; Giannoni et al., 2003). In these tests, the focus was on the response of cells to the applied cyclic loading. According to our simulations, the mechanical stimuli received by the cells is depth-dependent, a phenomenon that has not been considered in these previous tests.

During in vitro testing of cartilage explants, different loading conditions are applied to produce different

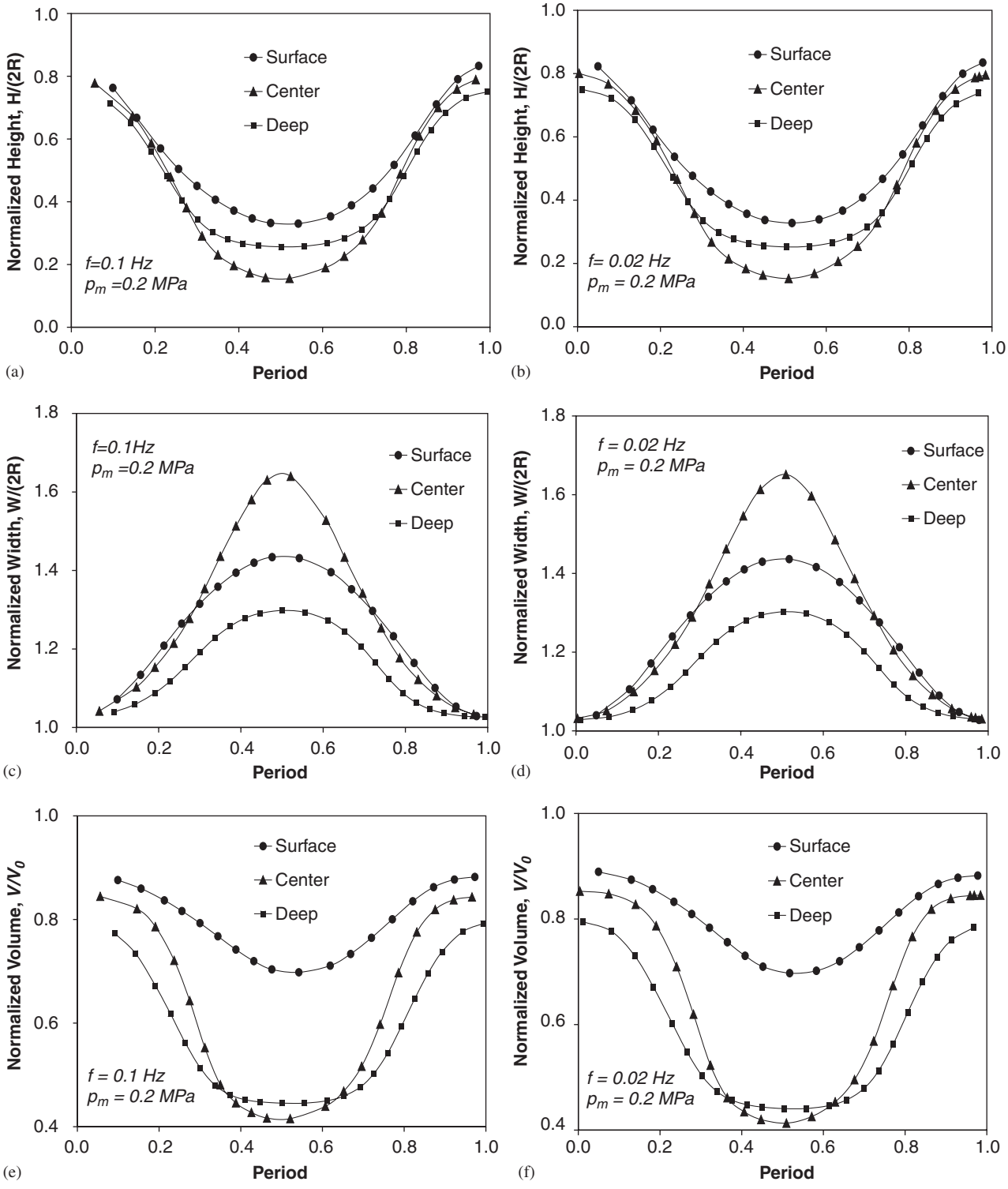

Fig. 5. Variations in cell shape for cyclic loading at $t = 1000$ s: $p_m = 0.2$ MPa. (a) and (b): normalized cell height, $f = 0.1$ and 0.02 Hz; (c) and (d): normalized cell width, $f = 0.1$ and 0.02 Hz; (e) and (f): normalized cell volume, $f = 0.1$ and 0.02 Hz. The cell volume as a function of time was normalized relative to that in the undeformed state, V_0; the cell height and cell width as a function of time was normalized relative to the cell diameter in the undeformed state, $2R$.

mechanical stimuli on the cells. According to our findings, changes in loading amplitude will not alter cell deformations proportionally across cartilage depth. The present simulations may be used as a guideline to predict the effect of load changes on cell deformations as a function of location.

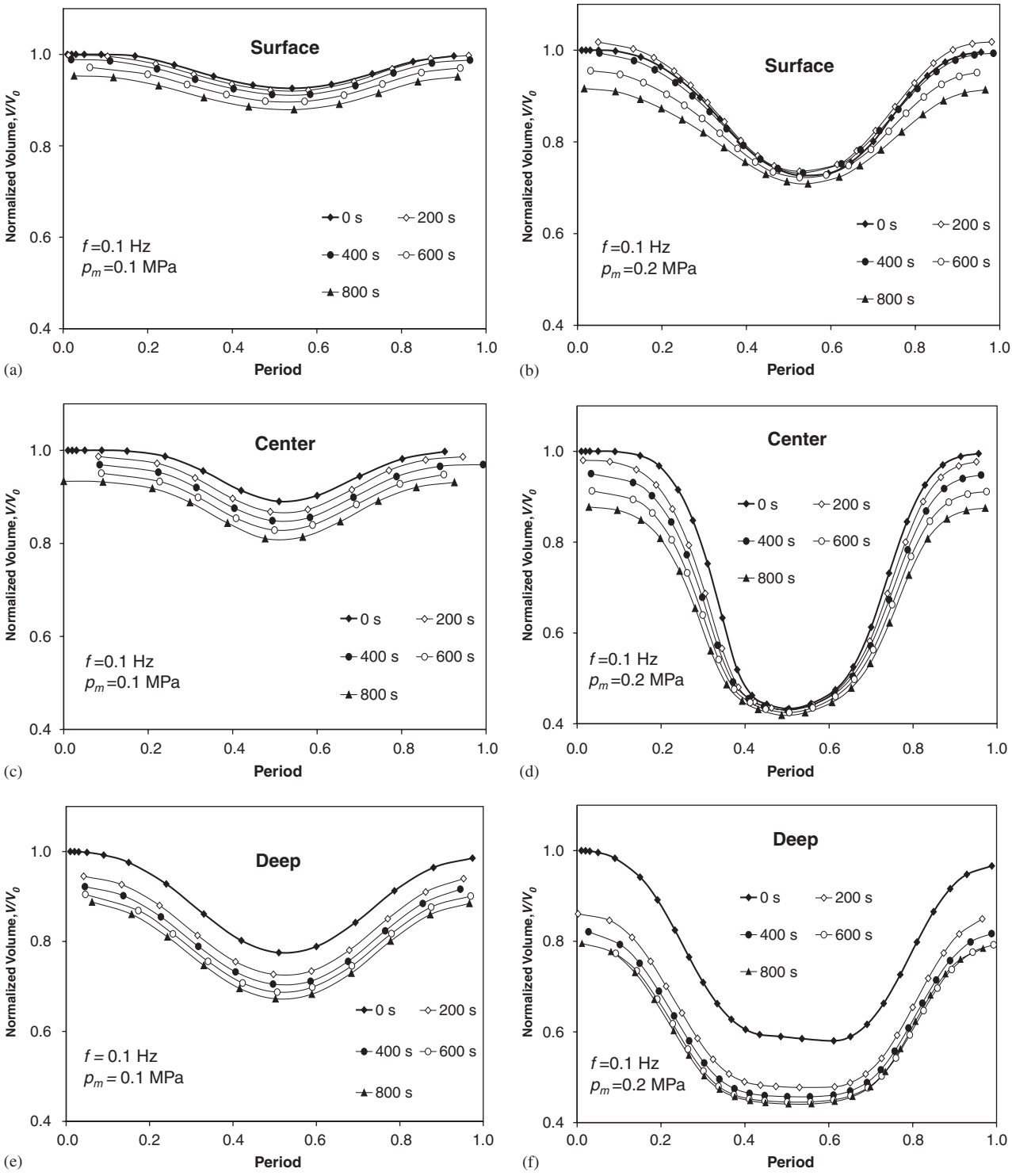

Fig. 6. Variations in cell volume as a function of time. (a) and (b): cell in the surface zone, $p_m = 0.1$ and 0.2 MPa; (c) and (d): cell in the middle zone, $p_m = 0.1$ and 0.2 MPa; (e) and (f): cell in the deep zone, $p_m = 0.1$ and 0.2 MPa. The cell volume as a function of time was normalized relative to that in the undeformed state, V_0.

In order to compare our simulation results with the experimental data by Knight et al. (1998), we re-plotted cell deformations for cyclic loading (Figs. 2–7; $f = 0.1$ Hz and $p_m = 0.1$ MPa) into time-histories, as shown in Fig. 9. We found that the magnitudes for cyclic cell deformations for these loading conditions are comparable with those obtained experimentally by Knight et al. (1998). The small differences between experiment and

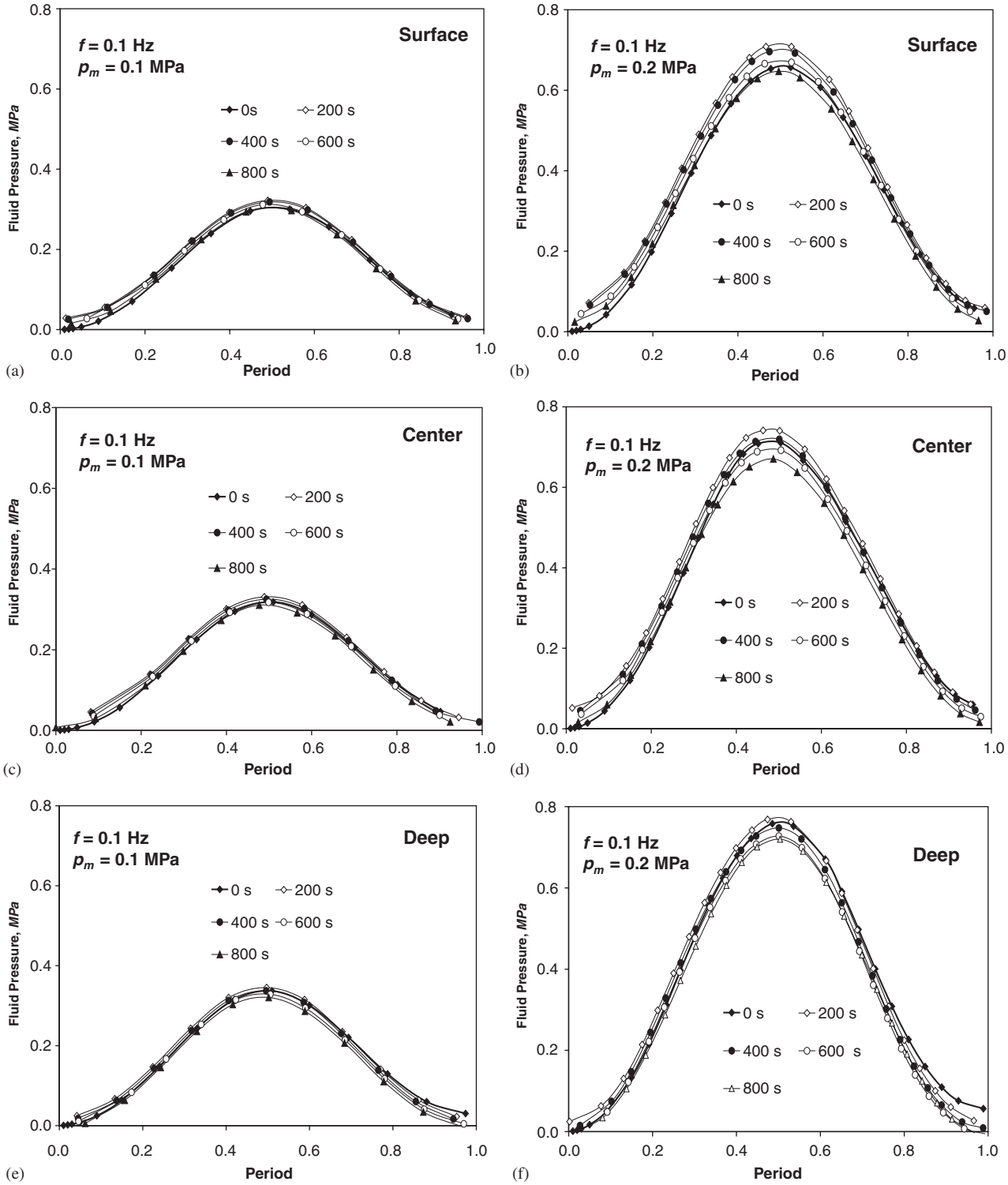

Fig. 7. Variations in hydraulic pressure at the center of the cell as a function of time for cyclic loading at $f = 0.1$ Hz. (a) and (b): cell in the surface zone, $p_m = 0.1$ and 0.2 MPa; (c) and (d): cell in the middle zone, $p_m = 0.1$ and 0.2 MPa; (e) and (f): cell in the deep zone, $p_m = 0.1$ and 0.2 MPa.

simulation are caused by differences in the loading conditions. Knight et al. (1998) compressed their cell-agarose samples in a displacement-controlled mode, while we simulated a load-controlled condition. Therefore, the comparison of our results to those obtained by Knight et al. (1998) is like comparing creep and stress relaxation tests.

Comparing our simulation results to the experimental observations by Guilak et al. (1995) and Guilak (1995),

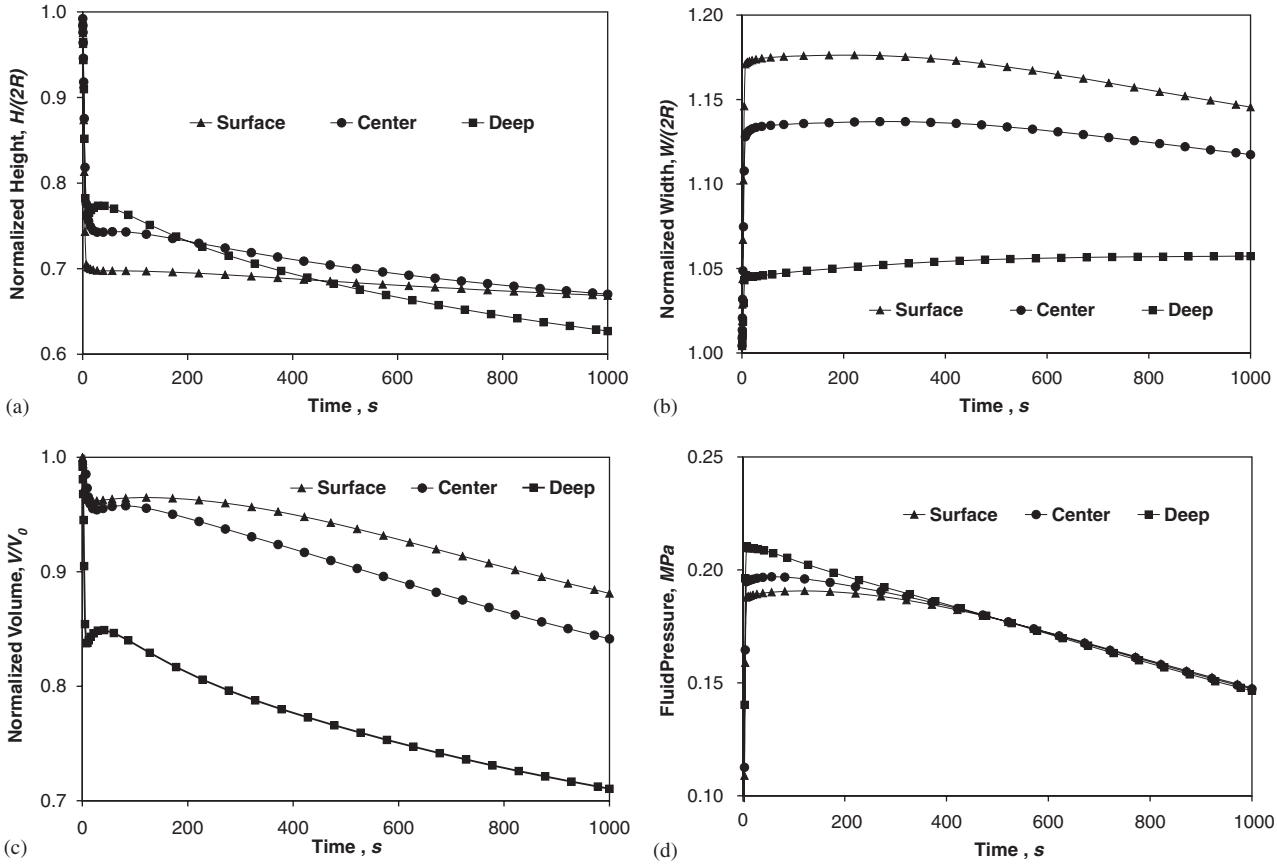

Fig. 8. Variations in cell shape and hydraulic pressure at the center of the cell as a function of time for static loading: $p = 0.14$ MPa. (a): normalized cell height; (b): normalized cell width; (c) normalized cell volume; (d) hydraulic pressure at the center of the cell. The cell volume as a function of time was normalized relative to that in the undeformed state, V_0; the cell height and cell width as a function of time were normalized relative to the cell diameter in the undeformed state, $2R$.

it becomes apparent that the deformation patterns predicted for the cyclic loading are different from those obtained for static loading. Guilak et al. (1995) and Guilak (1995) found that, at steady-state, chondrocyte height in the surface, middle, and deep layers decreased by 25.6%, 18.8%, and 20.7%; volume decreased by 21.8%, 15.5%, and 17.5%, respectively; and width increased by 1–4% after "steady-state" had been reached ($t = 1200$ s). For cyclic loading, we found that the chondrocytes in the surface zone experienced smaller deformations compared to those in the middle and deep zones, and increases in cell widths were more pronounced than those observed at steady-state.

Our simulation results suggest that the time-dependent deformation behavior of chondrocytes is coupled to the magnitude of the loading cycles. For large loading amplitudes ($p_m = 0.2$ MPa), the volumetric variations converged to steady-state values after about 20 loading cycles (Figs. 7b,d,f), while they did not reach steady-state values after 80 loading cycles for the small loading amplitude ($p_m = 0.1$ MPa) (Figs. 7a,c,e).

In the present simulations, the cells and the intracellular matrix were considered as biphasic porous media composed of a solid and a fluid phase. Since tissues' inertial effects are negligible at low frequency of cyclic loading, dynamic loading affects the deformations through the coupling of the interstitial fluid flow with the deformation of the solid phase. Since 70–80% of the load during the transient phase of dynamic loading is carried by the fluid phase (Park et al., 2003), fluid flow greatly influences the cartilage and chondrocyte deformations.

In our simulations, fluid pressure increased slightly from the superficial to the deep zone, while it decreased in the experiments by Park et al. (2003). This difference is likely caused by the difference in boundary conditions and the assumption of the cartilage properties in the simulations. While cartilage samples were compressed between two smooth platens in Park et al.'s (2003) study, the cartilage was fixed at the bottom and compressed through a smooth top platen in our simulations. The experimentally observed decrease in fluid pressure from the superficial to the deep zone is caused by a depth-dependent variation in strain which is associated with the tension-compression nonlinearity that has been observed in articular cartilage

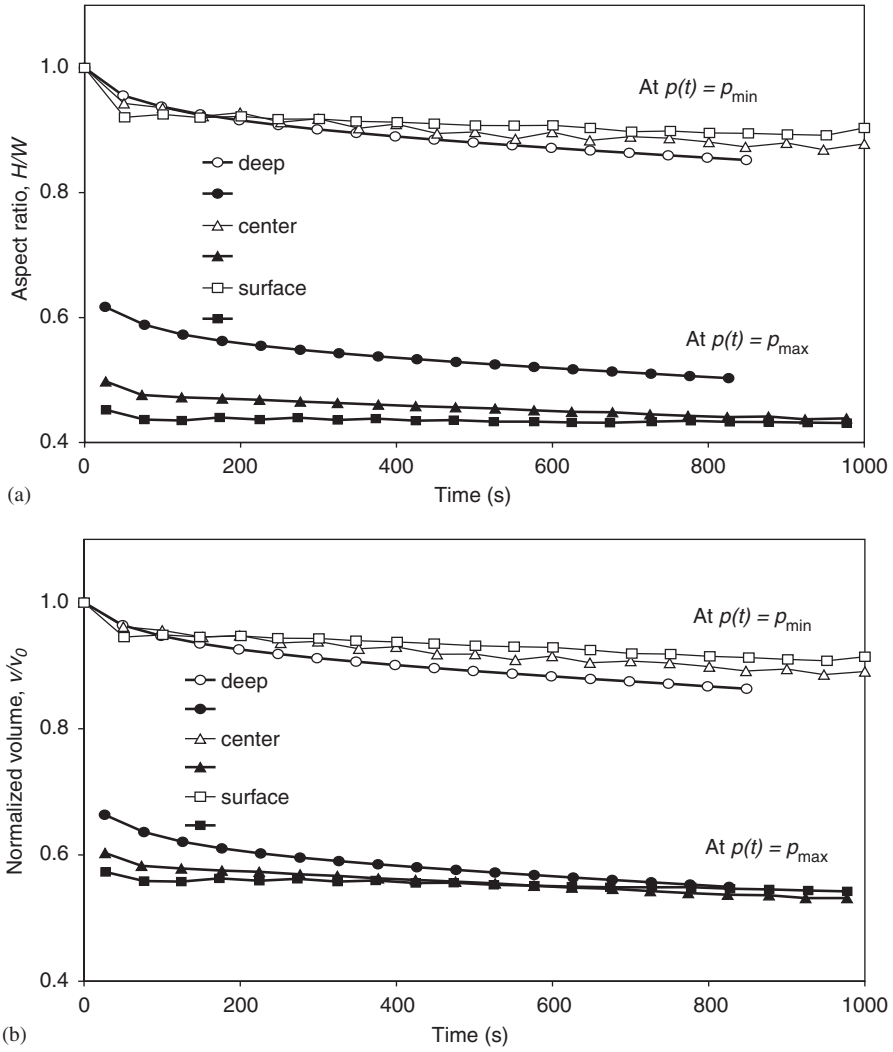

Fig. 9. Variations in shape and volume of cell during cyclic loading. (a): cell aspect ratio (width/height); (b): normalized cell volume. The cell volume was normalized relative to that in the undeformed state, V_0. The numerical tests were performed using $p_m = 0.1$ MPa and $f = 0.1$ Hz.

(Huang et al., 2003; Chahine et al., 2004). In our simulations, cartilage experienced greater strains in the superficial compared to the deep zone as the cartilage was perfectly fixed to the bottom platen. Since the stress in the solid phase was greater in the superficial compared to the deep zone, fluid pressure was greater in the deep compared to the superficial zone.

The major limitation of the present research is the assumption that the homogenized compressive modulus is constant throughout the cartilage layer. Also, it was assumed that the cells were spherical and uniformly distributed in the cartilage matrix, and most of the material properties were obtained from static tests. In real cartilage, cell shapes vary across zones (Clark et al., 2003), and the distribution of cells is not uniform (Wong et al., 1997). In the surface zone, cells are typically flattened; in the middle zone, cells are generally round (spherical); and in the deep zone, cells are characteristically arranged in columns. The average cell volumetric concentration decreases from the surface to the deep zone by a factor of about three (Wong et al., 1997). The pericellular matrix immediately surrounding chondrocytes has significantly different mechanical properties than isolated chondrocytes (Knight et al., 2001; Alexopoulos et al., 2003). The oriented, non-uniform distribution of the chondrocytes and other structural elements, such as the pericellular matrix and collagen network, will induce location-dependent, anisotropic mechanical properties of the homogenized cartilage matrix. The linear homogenization approach used in our model is not strictly valid for the large deformation problem solved here. Because all these effects were not included in the present model, readers should be cautious in generalizing results presented here to situations other than those simulated. Nevertheless, we expect that location-dependent cell deformations

observed here are valid, and likely would be exaggerated by the non-uniform stress/strain distributions experienced in a real joint, and the anisotropies present in real tissue.

In conclusion, our numerical simulations of the deformation behavior of chondrocytes in cyclic unconfined compression suggest that, in homogeneous cartilage layers, the mechanical response of chondrocytes to cartilage loading depends on time and location of the cells within the specimen. In physiological conditions, the mechanical environment of cells are more complex than simulated here because of the anisotropy, depth-dependent inhomogeneity, and tension compression non-linearity of the cartilage matrix. The present results are the first to suggest that deformations of chondrocytes at different depths may vary substantially by changing the applied loading amplitude.

Acknowledgements

The Arthritis Society of Canada, the Canadian Institutes for Health Research, and the Canada Research Chair Program are acknowledged for their financial support to the second author.

References

Alexopoulos, L.G., Haider, M.A., Vail, T.P., Guilak, F., 2003. Alterations in the mechanical properties of the human chondrocyte pericellular matrix with osteoarthritis. Journal of Biomechanical Engineering 125 (3), 323–333.

Ateshian, G.A., Warden, W., Kim, J., Grelsamer, R., Mow, V., 1997. Finite deformation biphasic material properties of bovine articular cartilage from confined compression experiments. Journal of Biomechanics 30, 1157–1164.

Athanasiou, K.A., Rosenwasser, M.P., Buckwalter, J.A., Malinin, T.I., Mow, V.C., 1991. Interspecies comparisons in in situ intrinsic mechanical properties of distal cartilage. Journal of Orthopaedic Research 9, 330–340.

Buschmann, M., Gluzband, Y., Grodzinsky, A., Hunziker, E., 1995. Mechanical compression modulates matrix biosynthesis in chondrocyte/agarose culture. Journal of Cell Science 108, 1497–1508.

Chahine, N.O., Wang, C.C., Hung, C.T., Ateshian, G.A., 2004. Anisotropic strain-dependent material properties of bovine articular cartilage in the transitional range from tension to compression. Journal of Biomechanics 37 (8), 1251–1261.

Clark, A.L., Barclay, L.D., Matyas, J.R., Herzog, W., 2003. In situ chondrocyte deformation with physiological compression of the feline patellofemoral joint. Journal of Biomechanics 36 (4), 553–568.

Elder, S.H., Goldstein, S.A., Kimura, J.H., Soslowsky, L.J., Spengler, D.M., 2001. Chondrocyte differentiation is modulated by frequency and duration of cyclic compressive loading. Annals of Biomedical Engineering 29 (6), 476–482.

Giannoni, P., Siegrist, M., Hunziker, E.B., Wong, M., 2003. The mechanosensitivity of cartilage oligomeric matrix protein (comp). Biorheology 40 (1–3), 101–109.

Guilak, F., 1995. Compression-induced changes in the shape and volume of the chondrocyte nucleus. Journal of Biomechanics 28, 1529–1541.

Guilak, F., Ratcliffe, A., Mow, V., 1995. Chondrocyte deformation and local tissue strain in articular cartilage: a confocal microscopy study. Journal of Orthopaedic Research 13, 410–421.

Holmes, M., 1986. Finite deformation of soft tissue: analysis of a mixture model in uni-axial compression. ASME Journal of Biomechanical Engineering 108, 372–381.

Huang, C.Y., Soltz, M.A., Kopacz, M., Mow, V.C., Ateshian, G.A., 2003. Experimental verification of the roles of intrinsic matrix viscoelasticity and tension-compression nonlinearity in the biphasic response of cartilage. Journal of Biomechanical Engineering 125 (1), 84–93.

Islam, N., Haqqi, T.M., Jepsen, K.J., Kraay, M., Welter, J.F., Goldberg, V.M., Malemud, C.J., 2002. Hydrostatic pressure induces apoptosis in human chondrocytes from osteoarthritic cartilage through up-regulation of tumor necrosis factor-alpha, inducible nitric oxide synthase, p53, c-myc, and bax-alpha, and suppression of bcl-2. Journal of Cell and Biochemistry 87 (3), 266–278.

Jones, W., Ting-Beall, H., Lee, G., Kelley, S., Hochmuth, R., Guilak, F., 1997. Mechanical properties of human chondrocytes and chondrons from normal and osteoarthritic cartilage. Transactions of Orthopaedic Research Society 22 (1), 199.

Knight, M.M., Ghori, S.A., Lee, D.A., Bader, D.L., 1998. Measurement of the deformation of isolated chondrocytes in agarose subjected to cyclic compression. Medical Engineering and Physics 20 (9), 684–688.

Knight, M.M., Ross, J.M., Sherwin, A.F., Lee, D.A., Bader, D.L., Poole, C.A., 2001. Chondrocyte deformation within mechanically and enzymatically extracted chondrons compressed in agarose. Biochimica Biophysica Acta 1526 (2), 141–146.

Kurz, B., Jin, M., Patwari, P., Cheng, D.M., Lark, M.W., Grodzinsky, A.J., 2001. Biosynthetic response and mechanical properties of articular cartilage after injurious compression. Journal of Orthopaedic Research 19 (6), 1140–1146.

Lucchinetti, E., Adams, C.S., Horton, W.E.J., Torzilli, P.A., 2002. Cartilage viability after repetitive loading: a preliminary report. Osteoarthritis Cartilage 10 (1), 71–81.

Mow, V.C., Kuei, S.C., Lai, W.M., Armstrong, C.G., 1980. Biphasic creep and stress relaxation of articular cartilage: theory and experiment. ASME Journal of Biomechanical Engineering 102, 73–84.

Nerucci, F., Fioravanti, A., Collodel, G., Gambera, D., Carta, S., Paccagnini, E., Bocchi, L., Marcolongo, R., 1999. Effect of hydrostatic pressure on morphological and ultrastructural aspects of normal and osteoarthritic human articular chondrocytes. Bollettino Della Societa Italiana di Biologia Sperimentale 75 (9–10), 55–62.

Park, S., Krishnan, R., Nicoll, S.B., Ateshian, G.A., 2003. Cartilage interstitial fluid load support in unconfined compression. Journal of Biomechanics 36 (12), 1785–1796.

Parkkinen, J.J., Ikonen, J., Lammi, M.J., Laakkonen, J., Tammi, M., Helminen, H.J., 1993. Effects of cyclic hydrostatic pressure on proteoglycan synthesis in cultured chondrocytes and articular cartilage explants. Archives of Biochemistry and Biophysics 300 (1), 458–465.

Sauerland, K., Raiss, R.X., Steinmeyer, J., 2003. Proteoglycan metabolism and viability of articular cartilage explants as modulated by the frequency of intermittent loading. Osteoarthritis Cartilage 11 (5), 343–350.

Shin, D., Athanasiou, K., 1997. Biomechanical properties of the individual cell. Transactions of Orthopaedic Research Society 22 (1), 352.

Stockwell, R., 1979. Biology of Cartilage Cells. Cambridge University Press, Cambridge.

Wong, M., Wuethrich, P., Buschmann, M., Eggli, P., Hunziker, E., 1997. Chondrocyte biosynthesis correlates with local tissue strain in

statically compressed adult articular cartilage. Journal of Orthopaedic Research 15, 189–198.

Wong, M., Siegrist, M., Cao, X., 1999. Cyclic compression of articular cartilage explants is associated with progressive consolidation and altered expression pattern of extracellular matrix proteins. Matrix Biology 18 (4), 391–399.

Wu, J.Z., Herzog, W., 2000. Finite element simulation of location- and time-dependent mechanical behavior of chondrocytes in unconfined compression tests. Annals of Biomedical Engineering 28 (3), 318–330.

Wu, J.Z., Herzog, W., Epstein, M., 1999. Modelling of location- and time-dependent deformation of chondrocytes during cartilage loading. Journal of Biomechanics 32 (6), 563–572.